The Society for engineering
in agricultural, food, and
biological systems

Paper Number: 033109
An ASAE Meeting Presentation

Robotic Simulation of the Docking and Path Following of an Autonomous Small Grain Harvesting System

Y. Hao

Ph.D. Student, Mechanical Engineering Department, University of Delaware

B. Laxton

Research Student, Computer and Information Sciences Department, University of Delaware

E.R. Benson

Assistant Professor, Delaware Experimental Station, Department of Bioresources
Engineering, College of Agriculture and Natural Resources, University of Delaware,
ebenson@udel.edu

S.K. Agrawal

Professor, Mechanical Engineering Department, University of Delaware

Written for presentation at the
2003 ASAE Annual International Meeting
Sponsored by ASAE
Riviera Hotel and Convention Center
Las Vegas, Nevada, USA
27- 30 July 2003

Abstract. *Researchers around the world have focused on autonomous agriculture, with systems encompassing greenhouse, orchard, field and other applications. Research has shown the potential and ability of the technology to allow a vehicle or selection of vehicles to follow a specified task. In this study, one aspect of the problem, that of operating a tractor-cart combination in conjunction with a small-grain combine harvester, was investigated. The tractor-cart combination and combine harvester application was selected because of the high fatigue and long duration aspects of the problem. The system was simulated using two iRobot Magellan Pro robots in an indoor environment. The differential drive robots were software constrained to match the dynamics of typical agricultural vehicles. Position feedback was supplied by odometry. A small towed trailer was added to one robot to simulate a typical grain cart.*

Keywords. automatic control, combine harvesters, computer simulation, farm machinery, farm management, model validation, modeling,

Introduction

Over the last 100 years, agriculture has made significant advances. Revolutions in mechanization, infotronics and genomics have increased yields. The combine harvester is a critical element in the harvesting of important field crops in North America. Combine size and capacity has increased to meet yield and management changes.

Research groups in the United States and internationally have begun to develop robotic systems for agriculture (Reid, 2000a and 2000b; Noguchi, et al., 1997). The majority of the projects have dealt with the development of robotic control systems and navigation systems for single agricultural vehicles, primarily tractors. Tractors are used for a wide variety of tasks, including tillage, planting, cultivation and harvest support. Researchers have begun to investigate harvester guidance systems, however, the state of the art has not reached that of the tractor guidance systems (Callahan, et al., 1997; Fitzpatrick, et al., 1997; Benson, et al., 2002). In the field, the harvesters operate in conjunction with one or more grain carts.

The grain cart travels from one or more harvesters in the field to the road transport or grain storage areas. Portions of the cart movement are done independently, away from other vehicles. When transferring harvested grain, the cart must move in formation with the harvester. The dimensions of the combine and cart require precision operation of both vehicles. The continuous operation and precision required for transfer are fatiguing.

The cart and harvester interactions are governed primarily by the harvester. During harvest, the primary object is to harvest the maximum quantity at the highest quality with a minimum of inputs (fuel, time, labor, etc). To achieve the maximum quantity in the minimum time, an overriding objective is to keep the harvesters operating at maximum effectiveness during the entire process. The grain cart has to sequence transfer and movement operations to prevent any or all harvesters in the field from reaching capacity (forcing a stoppage) before the cart can arrive. The cart has to select the appropriate harvester, based on distance and time to fill, locate the harvester using a combination of local and/or global sensors, travel to the harvester and travel in formation with the harvester as grain is transferred. After completion of the transfer, the cart is free to travel to other harvesters or return to an in-field storage station (typically a tractor trailer).

Current research has not concentrated on the cart and harvester interactions. Portions of the grain cart, tractor and harvester interactions can be developed from formation control of mobile robots (Hao, et al., 2003; Guo, et al., 2002; Fredslund, et al., 2001; Balch and Arking, 1998). Algorithms for control and coordination of the harvester and cart must account for the dynamic nature of the environment in which they operate (Pledgie, et al., 2002; Desai, 1998). The control of a single robot with a trailer has been investigated extensively (Lamiaraux and Laumond, 1998; Sekhavat, et al., 1997). Combining formation planning and control of mobile robots with trailers is a challenging problem.

Objectives

The general objective of the project was to develop a robotic simulation of formation following during the grain transfer process during combine harvesting. Within the general objective, two specific objectives were:

1) Develop a framework for development and testing of agricultural vehicle formation and docking strategies

2) Use the developed framework to test and evaluate specific strategies.

Project Description and Framework:

In this paper, we propose a practical framework for on-line planning and control of multiple mobile robots with trailers moving in groups. The group is trailer-centered and must maintain some predetermined geometric shape while moving and is allowed to change formation as necessary to negotiate through the environment. The combine path dictates the path of the trailer to ensure a collision free path that will allow grain transfer. The path of the trailer, in turn, dictates the required path of the tractor to ensure that the trailer is in the optimal location at the correct time.

We will use the ideas of differential flatness to plan and optimize trajectories for the mobile robot with trailers. Systems that exhibit the property of differential flatness were first studied by Fliess, et. al. (1995). Differential system $\dot{x} = f(x,u)$, where *x* is an *n*-dimensional vector of states and *u* an *m*-dimensional vector of control, is differentially flat if there exists variables *y* of the same dimension as the number of controls, so that states and inputs can be algebraically expressed in terms of *y* and its higher-order derivatives, i.e., $[x,u] = F(y, y^{(1)}, ..., y^{(p)})$.

Differentially flat systems are well suited to problems requiring trajectory generation. Since the outputs of a flat system completely describe its behavior, the trajectory can be planned in output space and the inputs that will cause the system to follow this trajectory can be calculated directly. The various aspects of flatness based optimal planning have been pursed (Fossas, et al., 2000; Ferreira and Agrawal, et al., 1999). Preliminary results of flatness based planning of groups of autonomous vehicles were reported in Pledgie, et al. (2002).

Trailers can be attached at the kingpin centered on the rear axle or on a hitch positioned behind the rear wheels (Figure 1). In the case of a tractor-trailer system with the point of rotation centered on the rear axle, the system is differentially flat. In the case of a hitch positioned behind the rear axle, the system is differentially flat for one trailer. Although agricultural tractors normally utilize hitches positioned behind the axle, this paper will concentrate on kingpin systems.

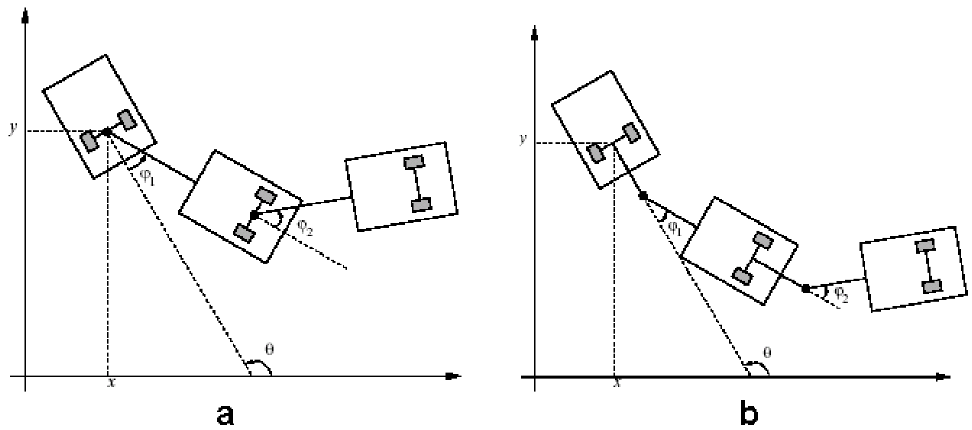

Figure 1. Two types of mobile robots with trailers

Planning and Control

A flow chart for formation planning and control is shown in Figure 2. In this project, the combine operator was assumed to provide the path, either from a GPS-based planting map or from on-board sensors. The combine path was reduced to a series of waypoints and the trajectory generator produces a continuous time trajectory for it. Then, according to the trailers' positions in the formation with respect to the virtual leader, the reference trajectories for trailers and real robots are generated. If there is a possible collision in the computed trajectories, the trailers' and robots' trajectories will be optimized given the reachable area for the trailers if a solution exists. Next, each robot tracks its own trajectory. Based on trailer stability analysis, if the robot tracks its reference trajectory well, the trailers attached to the robot will also converge to their own reference trajectories (Lamiraux and Laumond, 1998).

Robots obtain position feedback through odometry readings. If the environment doesn't change and there are no collisions between robots after trajectory optimization, the robots track their computed trajectories. If the environment changes or no solution is found to avoid collisions between robots, a new path and trajectory is generated and tracked by the controller.

Trailer and follower trajectory generation uses the flatness property of the system. For the formation group, the flat output is the combine's trajectory (x_c, y_c). Given the leader's trajectory, the last trailer's nominal trajectory will be determined geometrically. Other trailers and the follower robot's trajectories will be determined recursively. Collision-free trajectories between the combine and trailer can be guaranteed if the offset is carefully chosen. However, there could be collisions between the combine and the cart. These interformation collisions can be accounted for if there is some flexibility in the trailer's trajectories.

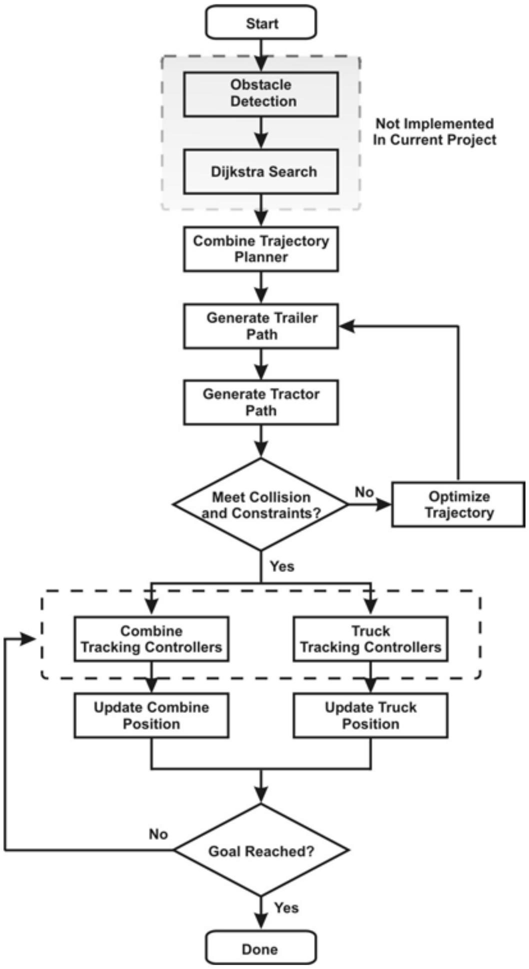

Figure 2. Flow chart for formation planning and control

The group G consists of *N* similar units and the dynamics of the *i*th unit is given by:

$$\dot{\bar{x}}_i = f(\bar{x}_i, u_i) \qquad i=1,...,N. \qquad (1)$$

Here, $\bar{x}_i \in \Re^n$ denote the states, $u \in \Re^n$ are the inputs and $f(\cdot)$ is a smooth mapping from its arguments. Trajectory planning for such a group consists of finding trajectories, which over a time horizon [t_0, t_f] satisfy the dynamic Eq. (1), the inequality constraints:

$$\bar{g}(x_1,...,x_N,t) \le 0, \bar{g} \in \Re^{n_g} \qquad (2)$$

$$\bar{c}(\bar{x}_1,...,\bar{x}_N,u_1,...,u_N,t) \le 0, \bar{c} \in \Re^{n_c} \qquad (3)$$

and specified terminal constraints, while minimizing a cost criterion given by:

$$\min \bar{J} = \Phi(\bar{x}_1(t_f),...,\bar{x}_N(t_f),t_f) + \int_{t_o}^{t_f} \bar{L}(\bar{x}_1,...,\bar{x}_N,u_1,...,u_N,t)dt \tag{4}$$

The inequality constraints involving configuration variables of the units in Eq. (2) have a well defined structure that comes from the organization of the group and the geometry of the formation. For this reason, they are distinguished from other inequality constraints on states and/or inputs in Eq. (3) and we call them configuration constraints. For example, during grain transfer, the combine and trailer need to stay within a minimum (collision) and maximum (failure to transfer) distance. Such constraints fall within the category of Eq. (2).

This trajectory optimization problem involves finding *N(n + m)* state and input trajectories in the presence of $n_g + n_c$ inequality constraints, while satisfying *Nn* state equations and given terminal constraints. The solution of such an optimization problem is known to be computationally demanding. In order to make this problem computationally more tractable and potentially solvable in close to real-time, the problem can be posed as multiple suboptimal problems that give some fixed forms and discretize the original continuous problem. If the resolution is small enough, the solution will be acceptable. Specifically, let's consider one tractor with a trailer that follows a combine time interval $[t_0, t_f]$. Let x_c and y_c denote the combine's x and y trajectories respectively. The heading angle θ_c can be calculated as follows:

$$\theta_c = \tan^{-1}\left(\frac{\dot{y}_c}{\dot{x}_c}\right) \tag{5}$$

Finally, the trailer's nominal trajectories (x_{tn} y_{tn}) can obtained by:

$$x_{tn} = x_c + dx * \cos(\theta_c) - dy * \sin(\theta_c) \tag{6}$$

$$y_{tn} = y_c + dx * \sin(\theta_c) - dy * \cos(\theta_c) \tag{7}$$

where dx and dy denote the trailer local position relative to the leader robot in the formation. Given flexibility in the trailer's motion, we can specify a circle around its nominal trajectory. A maximum permitted deviation distance (R) can be defined, in this case based on the dimensions of the grain cart. A suitable choice for the trajectory is polynomial such as $a_0 + a_1t + a_2t^2 + a_3t^3 + a_4t^4 + ...$ for the x trajectory and $b_0 + b_1t + b_2t^2 + b_3t^3 + b_4t^4 ...$ for the y trajectory. The coefficients $a_0, a_1, a_2..., b_0, b_1, b_2...$ are parameters. a_0, b_0 are determined by the current trailer's position and the nominal position at $t = t_0$. This way the trailer can be put anywhere in the feasible area and the trajectory will be continuous during map updating. Thus, the trailer's trajectory (x_t, y_t) is given as:

$$x_t = x_{tn} + a_0 + a_1t + a_2t^2 + a_3t^3 + a_4t^4 ... \tag{8}$$

$$y_t = y_{tn} + b_0 + b_1t + b_2t^2 + b_3t^3 + b_4t^4 ... \tag{9}$$

$$(a_0 + a_1t + a_2t^2 + ...)^2 + (b_0 + b_1t + b_2t^2 + ...)^2 < R^2 \tag{10}$$

The trailer's angle (θ_t) can be calculated as well.

$$\theta_t = \tan^{-1}\left(\frac{\dot{y}_t}{\dot{x}_t}\right) \tag{11}$$

The tractor pulls the trailer through the required trajectory. The tractor's trajectory (x_p y_p) can be computed by:

$$x_p = x_t + l * \cos(\theta_t) \tag{12}$$

$$y_p = y_t + l * \sin(\theta_t) \tag{13}$$

Where l is the distance between the midpoint of the tractor and trailer wheels.

The cost function is aimed to minimize the trailer's deviation from the nominal trajectory. In order to optimize in real-time, a finite discrete set (S) must be used. For example, a uniform discretization is $t_o + i\frac{t_f - t_0}{n}, i = 0,...n$. Each vehicle in the formation was reduced to a series of circular constraint points (Figure 3 (A)). For the tractor and combine, multiple constraint points were used to dictate the desired behavior and avoid collisions. Each constraint point included x and y coordinates and a radius of conformity. For collision avoidance, the radius was specified as a distance that other vehicles could not operate within. For grain transfer, the radius was specified as a distance that the combine discharge auger had to remain within. The radius constraints were dictated by vehicle geometry. On satisfying the constraints at the discrete points, the optimization problem becomes:

$$\min \; J = \max_{i=1...n}((a_0 + a_1\tau + a_2\tau^2 + a_3\tau^3 + a_4\tau^4 + ...)^2 + (b_0 + b_1\tau + b_2\tau^2 + b_3\tau^3 + b_4\tau^4 + ...)^2) \tag{14}$$

$$\text{s.t.} \quad (x_p - x_c)^2 + (y_p - y_c)^2 > d_{ij}^2 \qquad \forall \tau \in S$$

$$(a_0 + a_1\tau + ...)^2 + (b_0 + b_1\tau + ...)^2 < R^2, \; |\phi| < \frac{\pi}{3}, \; |\beta| < \frac{\pi}{3}$$

where d_{ij} is the safe distance between circle i and circle j, M and N are the approximation circle sets for the follower robot and leader robot respectively, ϕ is the tractor wheel angle and β is the tractor-trailer angle.

Given the desired optimized trajectory, a tracking controller was developed to ensure that the tractor correctly followed the correct trajectory. According to the proof in Lamiraux and Laumond (1998), if a robot tracks its reference trajectory well during forward motion, its trailer will also converge to its own reference trajectory. The lead vehicle (combine) dictates the path of the trailer; the path of the trailer in turn dictates the required path of the tractor to achieve the desired trailer trajectory. The computational process reverses the standard driving model in which the tractor dictates the trailer path.

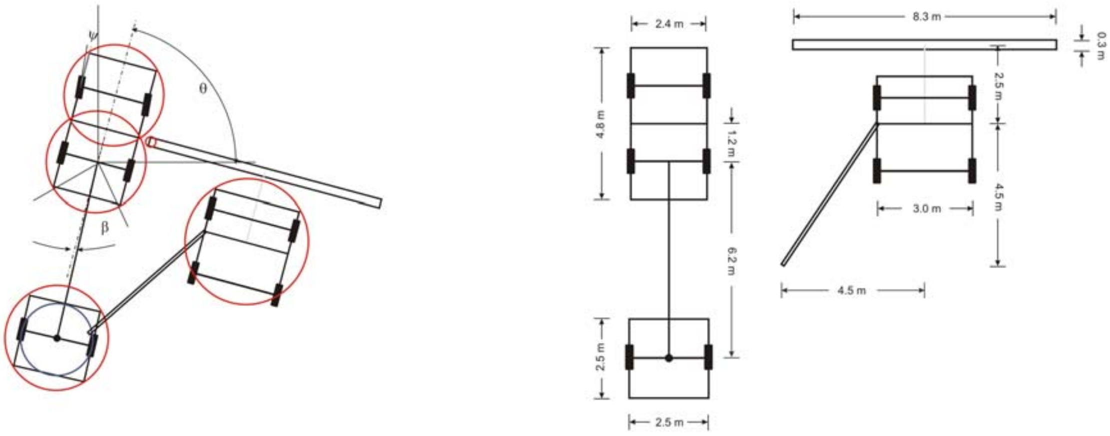

A. Vehicle constraint points B. Simulation dimensions

Figure 3. Vehicle constraint points and simulation dimensions

Corrective strategies are required to keep the vehicles on these trajectories. The equations of motion for a rear wheel drive tractor are governed as shown below: (Eqns. 15 to 18)

$$\dot{x}_i = u_{1i}\cos(\theta_i) \tag{15}$$

$$\dot{y}_i = u_{1i}\sin(\theta_i) \tag{16}$$

$$\dot{\theta}_i = \frac{u_{1i}}{l}\tan(\psi_i) \tag{17}$$

$$\dot{\psi}_i = u_{2i} \tag{18}$$

In the experiment, the mobile robot is driven by a simple differential drive, with two coaxial powered wheels and a passive supporting castor wheel. The robots used for the simulation and experiment are differential drive and are governed as shown: (Eqns. 19 to 21)

$$\dot{x}_i = u_{1i}\cos(\theta_i) \tag{19}$$

$$\dot{y}_i = u_{1i}\sin(\theta_i) \tag{20}$$

$$\dot{\theta}_i = u_{2i} \tag{21}$$

Here (x_i, y_i) denotes the position of the center of the axle with respect to the inertial frame and θ_i denotes the orientation of the vehicle in the inertial frame and β_i the angle between the tractor and trailer. The inputs to the controller are u_{1i} and u_{2i} which are the forward driving speed and angular speed of the robot. The actual front wheel angle (ψ) will be software constrained (Eqn. 22). The tracking controller from Samson et K. Ait-Abderrahim (1991) has been used here. If (x_r, y_r, θ_r) are the coordinates of the reference robot in the frame of the real robot, and if (u_{1i}^0, u_{2i}^0) are the inputs of the reference trajectory, this control law has the following expression:

$$\psi = \tan\left(\frac{u_{2i} l}{u_{li}}\right) < \frac{\pi}{3} \tag{22}$$

$$u_{1i} = u_{1i}^0 \cos(\theta_r) + k_1 x_r \tag{23}$$

$$u_{2i} = u_{2i}^0 + k_2 \frac{\sin(\theta_r)}{\theta_r} y_r + k_3 \theta_r \tag{24}$$

Methods and Materials

A physical implementation of the strategy for formation planning and control was performed to test the practicality of the concept. A schematic of the experimental setup is shown in Figure 4 (A). The setup consists of two differential drive iRobot[1] (Burlington, MA) Magellan Pro mobile robots where one has a trailer. One robot was designated as the leader (combine) and the second robot was designated as a tractor. A scratch built trailer was attached to the tractor robot, with vertical axis of the hitch passing through the midpoint of the drive axle (Figure 4 (A)). An angular encoder gives the absolute direction β of the trailer with respect to the direction of the tractor. Each robot has an on-board PC consisting of an EBX motherboard and a Pentium III processor. The robot operates under Linux operating system and its software integrates sensor and communication data. The robots communicate through wireless Ethernet capable of transmitting data up to 3Mb per second.

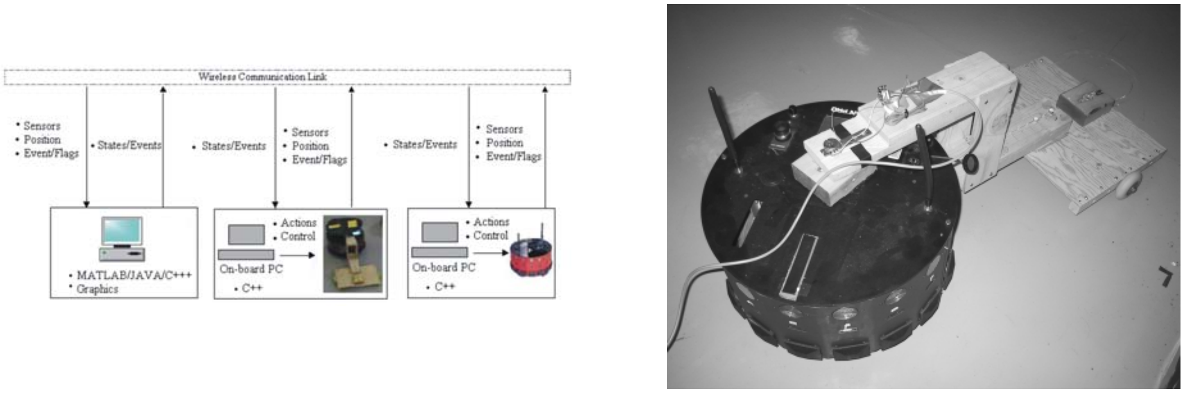

A. Schematic of the experimental setup

B. Trailer equipped iRobot

Figure 4. Experimental setup

---

[1] iRobot is a trademark of iRobot Corporation. Mention of trade name, proprietary product or specific equipment does not constitute a guarantee or warranty by the University of Delaware, and does not imply the approval of the named product to the exclusion of other products that may be suitable.

Translational and rotational velocity controllers are used to reposition each robot. MATLAB/C++/JAVA are used as the computational engine for decision making, control and graphical display. A version of CFSQP optimization program is used (Lawrence, et al., N/A).

The purpose of the experiment is to show that these algorithms work in real-time for trajectory generation, optimization and sensor updating in a dynamic environment. A block-diagram of the computational procedure is shown in Figure 5. Our experiment consisted of a leader robot (combine) and a follower robot-trailer combination (tractor and cart).

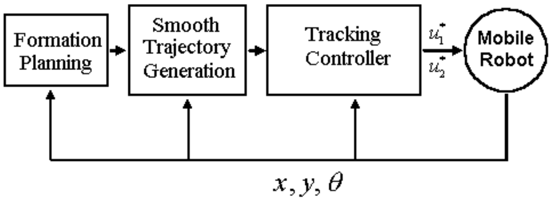

Figure 5. Formation planning and tracking control

Experimental Results

A sample agricultural setting was simulated both in software and using the experimental hardware. Simulation dimensions were established to mimic typical agricultural vehicles (Figure 3 (B)). The vehicle dimensions were scaled to 10% for the simulations. Vehicles modeled in the simulation included were a John Deere 8120 MFD tractor pulling a J&M 1075 cart and a John Deere 9650 STS combine with a 8 row corn head. The combine pathway was preselected, arbitrary and harsher than expected for a typical agricultural setting. The combine was assumed to exactly follow the pathway.

The formation following ability was modeled in C/C++ and the data processed in Mathworks MATLAB. The algorithm was able to develop an optimal path to ensure a collision free trajectory, reasonable rotation angles and that the combine discharge auger was within the cart for the entire pathway. The running time for one loop including optimization was 0.9 s (1.11Hz). There are eight parameters to optimize. In the experiment, the parameters are calculated first. If there are no changes in the environment, the parameters are not recalculated. The running time for one loop is 0.144 s (6.94 Hz). Pre-optimization and post-optimization trajectories are shown in Figure 6.

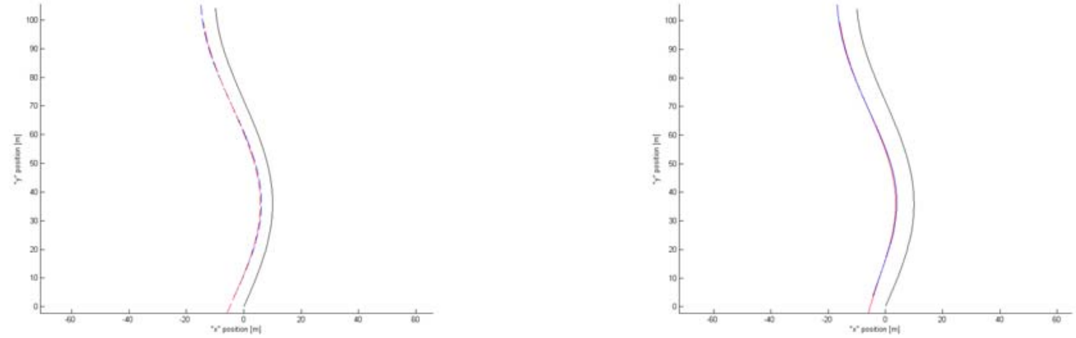

A. Pre-optimization trajectories B. Post-optimization trajectories

Figure 6. Combine, tractor and trailer trajectories

The optimization considered multiple vehicle constraints. Vehicle constraints included a) ensuring no collisions; b) maximum possible steering angles of ± 60º; and c) maximum trailer hitch angles of ± 60º. Auger to trailer center distance (Figure 7 (A)) was within the 2.5 m radius specified by trailer dimensions, illustrating that the auger discharge remained above trailer for the entire simulation. A time history of the tractor steering angle is shown in Figure 7 (B). The tractor angle stays within the specified range.

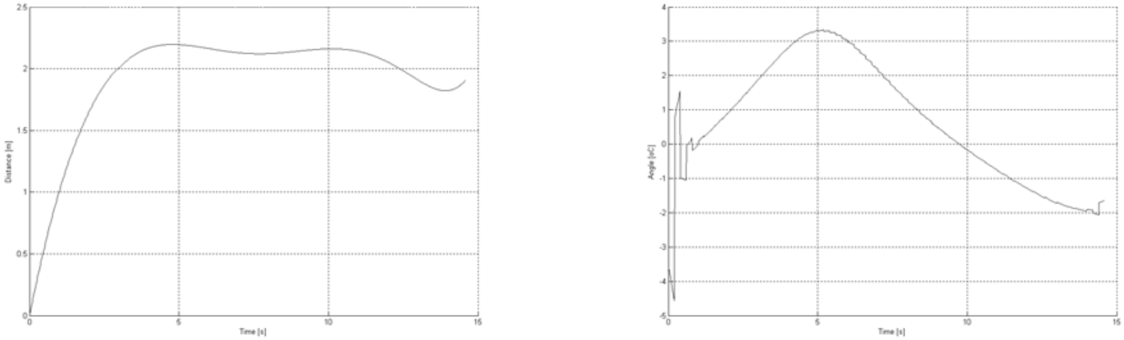

A. Auger to trailer center distance B. Tractor steering angle

Figure 7. Vehicle constraint plots

Overhead views of the vehicles were plotted out at various points during the simulation. Sample overhead simulation plots are shown in Figure 8 (A) and 8 (B).

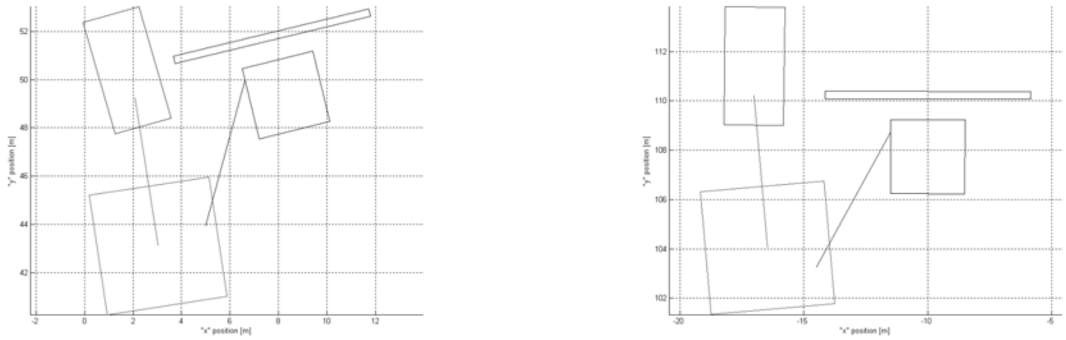

t = 6.3 s t = 15.0 s

Figure 8. Snapshot sequences in the simulation, showing the positions of the vehicles at various instances in time.

After simulating the algorithm in C/C++ and MATLAB, iRobot Magellan Pro robots were used to test the concept. The combine discharge auger, header and trailer were added to the to Magellan Pro robots to better simulated the agricultural system. The dimensions of the physical simulation were approximately 10% of the real world system. A sample image from the robotic simulation is shown in Figure 9 (A). The optimized reference and actual robot trajectories are shown in Figure 9 (B). Videos of the robotic simulation are available at: *http://mechsys4.me.udel.edu.*

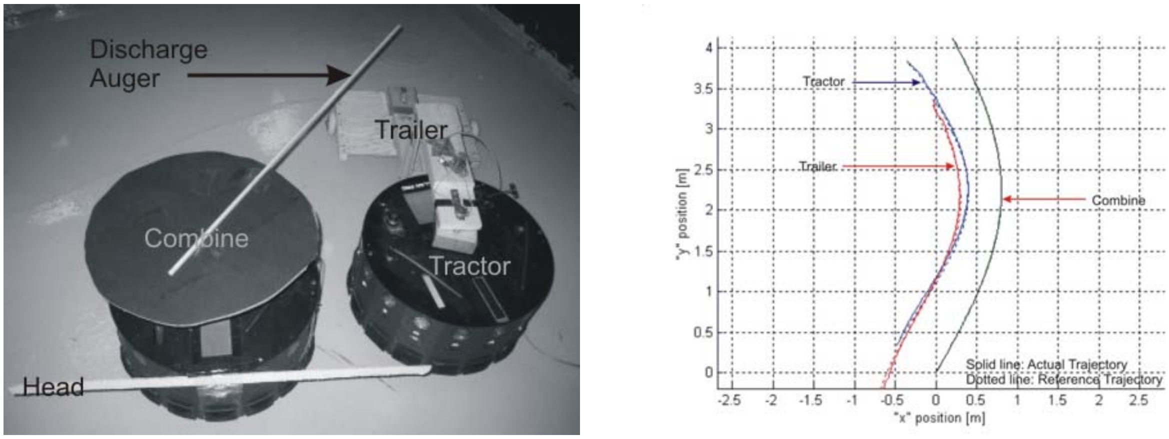

A. Robotic simulation B. Reference and actual robot trajectories

Figure 9. Sample images from the robotic simulation

From the results of this experiment, it is clear that the algorithms are feasible to implement real-time responsive behavior with currently available hardware.

Conclusion

Researchers around the world have developed individual robotic vehicles for agriculture. The interface or coordination of fleets of agricultural robotic vehicles has not been investigated as extensively. In this project, the movement of a combine and tractor-cart combination was modeled. The tractor-cart combination and combine harvester application was selected because of the high fatigue and long duration aspects of the problem An optimization procedure was developed to create an appropriate path to satisfy performance objectives and constraints. The algorithm was validated through computer simulations and iRobot Magellan Pro robots. The differential drive robots were software constrained to match the dynamics of typical agricultural vehicles. Position feedback was supplied by odometry. A small towed trailer was added to one robot to simulate a typical grain cart.

Acknowledgements

The authors acknowledge the research support of the University of Delaware College of Agriculture and Natural Resources, the National Science Foundation (Award # IIS-9912447) and National Institute of Standards (Award # 60NANB2D0137). We acknowledge the use of CFSQP program provided by University of Maryland.

References

Balch, T., and R.C. Arkin. 1998. Behavior-based Formation Control for Multi-robot Teams. *IEEE Transactions on Robotics and Automation.* 14: 926-939.

Benson, E.R., J.F. Reid, and Q. Zhang. 2001. “Machine Vision Based Steering System for Agricultural Combines.” ASAE Paper No. 01-1159. St. Joseph, MI: ASAE.

Callaghan, V., P. Chernett, M. Colley, T. Lawson, J. Standeven, M. Carr-West and M. Ragget. 1997. Automating agricultural vehicles. *Industrial Robot*. 24(5): 364-369.

Desai, J.P., J. Ostrowski, and V. Kumar. 1998. *Controlling formations of multiple mobile robots. Proceedings of IEEE International Conference on Robotics and Automation.* Leuven, Belgium.

Ferreira, A.M., and S.K. Agrawal. 1999. Planning and Optimization of Dynamic Systems via Decomposition and Partial Feedback Linearization. *Proceedings of the 38th Conference on Decision and Control*. Arizona.

Fitzpatrick, K., D. Pahnos and W.V. Pype. 1997. Robot windrower is first unmanned harvester. *Industrial Robot.* 24(5): 342-348.

Fliess, M., J. L´evine, P. Martin and P. Rouchon. 1995. Flatness and Defect of Non-linear Systems: Introductory Theory and Examples. *International Journal of Control.* 61(6): 1327-1361.

Fossas, E., J. Franch, and S.K. Agrawal. 2000. Linearization by prolongations of two-input driftless systems. *Proceedings of the 39th CDC*. Sidney.

Guo, Y., and L.E. Parker. 2002. A Distributed and Optimal Motion Planning Approach for Multiple Mobile Robots. *Proceedings of IEEE International Conference on Robotics and Automation.* Washington, DC.

Hao, Y., Laxton, B., Agrawal, S.K., Lee, E., Benson, E., 2003. Planning and Control of UGV Formations in a Dynamic Environment: A Practical Framework with Experiments. *Proceedings of IEEE International Conference on Robotics and Automation.* Taibei, Taiwan.

Lamiraux, F. and J.P. Laumond. 1998. A practical approach to feedback control for a mobile robot with trailer. *Proceedings of IEEE International Conference on Robotics and Automation.* Leuven, Belgium.

Lawrence, C. Zhou, J.L. and Tits, A. 2002. User's Guide for CFSQP Version 2.5: A C Code for Solving (Large Scale) Constrained Nonlinear (Minimax) Optimization Problems, Generating Iterates Satisfying All Inequality Constraints. *University of Maryland, College Park, MD.*

Noguchi, N., K. Ishii, and H. Terrao. 1997. Development of an agricultural mobile robot using a geomagnetic direction sensor and image sensors. *J. agric. Engng Res.* 67(1): 1-15.

Pledgie, S. T., Hao, Y., Ferreira, A. M., Agrawal, S. K., Murphey, R. 2002. Groups of Unmanned Vehicles: Differential Flatness, Trajectory Planning, and Tracking Control. *Proceedings of IEEE International Conference on Robotics and Automation.* Washington, DC.

Reid, J.F. 2000. Establishing automated vehicle navigation as a reality for production agriculture. *In Proc. 2nd IFAC/CIGR International Workshop on Bio-Robotics, Information Technology and Intelligent Control for Bioproduction Systems*, 33-40. Osaka, Japan, 25-26 November.

Reid, J.F., Q. Zhang, N. Noguchi and M. Dickson. 2000. Agricultural Automatic Guidance in North America. *Computers and Electronics in Agriculture* 25(1/2): 154-168.

Samson et K. Ait-Abderrahim, C. 1991. Feedback control of a nonholonomic wheeled cart in Cartesian space. *Proceedings of IEEE International Conference on Robotics and Automation*. Sacramento, California. 1136-1141.

Sekhavat, S., F. Lamiraux, J.P. Laumond, G. Bauzil, and A. Ferrand. 1997. Motion planning and control for Hilare pulling a trailer: experimental issues. *Proceedings of IEEE International Conference on Robotics and Automation.* Albuquerque, New Mexico.